

Thermophoresis: microfluidics characterization and separation

Daniele Vigolo,^a Roberto Rusconi,^b Howard A. Stone^{*c} and Roberto Piazza^{*d}

Received 2nd February 2010, Accepted 15th April 2010

DOI: 10.1039/c002057e

We show that thermophoresis, *i.e.*, mass flow driven by thermal gradients, can be used to drive particle motion in microfluidic devices exploiting suitable temperature control strategies. Due to its high sensitivity to particle/solvent interfacial properties, this method presents several advantages in terms of selectivity compared to standard particle manipulation techniques. Moreover, we show that selective driving of particles to the cold or to the hot side can be achieved by adding specific electrolytes and exploiting the additional thermoelectric effect stemming from their differential thermal responsiveness.

The development of efficient microfluidic separation and fractionation methods requires the design of novel and flexible approaches. A key figure of merit to assess the performance of a specific separation device is its selectivity. To this aim, usual methods such as electrophoresis^{1–3} or dielectrophoresis^{4–8} are not suitable to discriminate between particles or macromolecular solutes which, although functionally distinct, are similar in terms of size and charge. Moreover, when dealing with conductive aqueous suspensions, these methods suffer from the major drawback of Joule heating.⁹ Similarly, methods exploiting acoustic waves,¹⁰ hydrodynamic fields,¹¹ or optical properties,¹² which rely on basic physical bulk properties of the particles, lack any chemical specificity, which is often a crucial issue for tagging biological samples with superparamagnetic beads^{13–15} and driving them by magnetophoresis.

Selectivity could be better achieved by exploiting effects whose underlying physical mechanisms depend on specific particle/solvent interactions. The main aim of this work is to show that thermophoresis, which refers to particle transport driven by thermal gradients, fully meets this goal, and can therefore be effectively used as a selective particle separation method in simple microfluidic devices. We shall also show that tuning of the strength and even of the direction of particle drift can be attained by controlling the solvent composition, in particular by adding thermally responsive electrolytes.

We first briefly review the basic phenomenon based description of thermophoresis, which is akin to thermal diffusion, or the Soret effect, in simple fluid mixtures.¹⁶ As we stated, thermophoresis is an additional particle transport mechanism brought in, on top of Brownian diffusion, by the presence of a thermal gradient. We can then write the total mass flux as

$$\mathbf{J} = -D\nabla c - cD_T\nabla T \quad (1)$$

where D is the usual Brownian diffusion coefficient. For historical reasons, related to the study of thermal diffusion in simple liquid mixtures, D_T is generally called the thermal diffusion coefficient. Dimensionally, however, D_T is *not* a diffusion coefficient and, noting that the steady-state thermophoretic velocity acquired by the particle is given by $\mathbf{v}_T = -D_T\nabla T$, it should rather be called thermophoretic mobility, in analogy with other transport effects such as electrophoresis. Observing that the “thermodynamic force” associated with a thermal gradient is actually $\nabla T/T = \nabla \ln(T)$, an alternative definition can be given by writing the mass flux per unit concentration $\mathbf{J}' = \mathbf{J}/c$ as

$$\mathbf{J}' = -D\nabla \ln(c) - \tilde{D}_T\nabla \ln(T) \quad (2)$$

where $\tilde{D}_T = TD_T$ is a *true* diffusion coefficient that can effectively be compared with D .

If ∇T is applied to a dilute suspension confined between two parallel plates the system reaches, in the absence of convection, a steady-state concentration gradient:

$$\nabla c = -cS_T\nabla T \quad (3)$$

where $S_T = D_T/D$ is called the Soret coefficient. According to eqn (3), when $S_T > 0$ particles move to the cold side, and the suspension is usually called thermophobic, while the opposite (less frequent) behavior is referred to as thermophilic. Within the restricted geometry of a microfluidics device, convective effects are expected to be totally negligible. Therefore, if a temperature difference ΔT is applied across a channel of width w , and provided that S_T can be taken as temperature-independent within the range ΔT , the steady-state concentration c_h at the hot plate is related to its value c_c close to the cold plate by

$$c_h = c_c \exp(-S_T\Delta T) \quad (4)$$

Therefore, if $S_T\Delta T \ll 1$, a relative concentration difference $\Delta c/c = -S_T\Delta T$ between the hot and the cold wall is reached in a time scale $\tau \approx w^2/(\pi^2 D)$.

In recent years, a large number of experimental studies have been devoted to investigate thermophoretic effects for a wide class of colloidal systems and complex fluids, ranging from latex particle suspensions, to polymer and surfactant solutions, to biological fluids (for a comprehensive review, see ref. 16). These

^aDepartment of Chemistry, Material Science, and Chemical Engineering, Politecnico di Milano, 20133 Milano, Italy

^bSchool of Engineering and Applied Sciences, Harvard University, Cambridge, MA, 02138, USA

^cDepartment of Mechanical and Aerospace Engineering, Princeton University, Princeton, NJ, 08544, USA. E-mail: hastone@Princeton.edu

^dDepartment of Chemistry, Material Science, and Chemical Engineering, Politecnico di Milano, 20133 Milano, Italy. E-mail: roberto.piazza@polimi.it

investigations have unraveled several general features of particle thermophoresis. First, although the Soret coefficient varies very widely depending on the nature and size of the colloidal particles, for most systems the thermophoretic mobility varies within the fairly limited range $1 < D_T < 10 \mu\text{m}^2 \text{s}^{-1} \text{K}^{-1}$. This range of values sets precise limits for the separation efficiency of a device. Second, the specific values of D_T and S_T depend very much on the thermodynamic conditions of the suspension, and in particular on the average temperature. By increasing T , indeed, most investigated aqueous colloids switch from thermophilic to thermophobic at a temperature T^* which is system-dependent, and follow a rather universal trend.¹⁷ Third, this peculiar feature, which stems from the interfacial nature of the thermophoretic effect,¹⁶ can be profitably exploited in separation methods. For example, two biological macromolecules with similar molecular weight and charge may have sufficiently different values of T^* to be driven in opposite directions by carefully tuning the working temperature.¹⁸ A final recent observation,^{19,20} which will be exploited in this paper, is that the addition of specific electrolytes displaying particular ionic thermal diffusion leads to the buildup of a steady-state electric field, which can hinder or conversely enhance the particle thermophoretic drift. These thermoelectric phenomena allow tuning the value of T^* , and therefore the direction of particle motion.

Micro-separators exploiting custom solutions, where controlled thermal gradients can be applied, have already been proposed and tested successfully.^{22,23} Practical devices based on standard soft-lithography techniques^{24,25} may however offer greater flexibility in geometrical design and fabrication. Nevertheless, they require specific solutions for imposing, controlling, and measuring thermal gradients on the microfluidics scale. To this aim, we have contrasted two different approaches, where thermal control is respectively achieved by circulation of water or by ohmic heating of a channel adjacent to the test channel. In both cases, we have fabricated microfluidic devices made of polydimethylsiloxane (PDMS) sealed onto a standard cover-glass of thickness $d = 0.17 \text{ mm}$, where co-running side channels are used as hot and cold thermal sources for a central sample channel. Such a design allows for direct optical inspection of the flow. We manufactured several devices, which are $25 \mu\text{m}$ deep, varying the width w of the sample channel between 50 and $100 \mu\text{m}$. The channel is separated by a PDMS layer about $100 \mu\text{m}$ thick from the much wider (2 mm) side channels (see Fig. 1a). The temperature is monitored using two thermistors stuck to the cover glass by thermal grease and insulated by a PDMS layer. As PDMS has a much lower thermal conductivity ($k_P = 0.15 \text{ W/mK}$) than water ($k_w = 0.6 \text{ W/mK}$), a large part of the detected temperature difference ΔT_0 occurs across the PDMS layer separating the side from the sample channels.

The first design consists of introducing two additional lateral chambers, about 5 mm wide, where hot water coming from a thermostatic bath and room-temperature tap water are, respectively, circulated at high flow rates (Fig. 1a). One disadvantage of this solution is that it does not allow for a convoluted sample channel design. As discussed in detail in ref. 21, our alternative strategy consists in directly embedding a resistive heater into the device by filling one of the side channels with a silver-laden bi-component epoxy adhesive (Epo-Tek®H20S). The other side of the test channel is kept cool by flowing cold

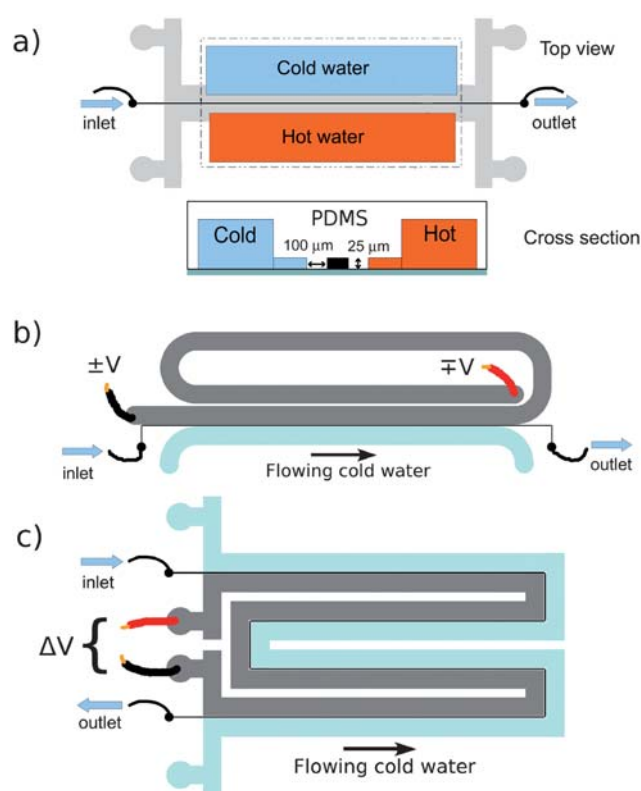


Fig. 1 (a) A microfluidic device where temperature gradients are established by flowing hot and cold water. Side channels and reservoirs, together with the sample microchannel, are shown in the cross-sectional view. (b) An alternative design where the hot water channel is replaced by a silver-epoxy resistive heater. The sample channel for the devices shown in (a) and (b) is 40 mm long. (c) A device using an embedded ohmic heater as in (b), but with a longer path (120 mm long). For technical details, see ref. 21.

water at high rate (typically $800 \mu\text{L min}^{-1}$) by means of a syringe pump. The crucial advantage of using this conductive epoxy is that, due to its moderate viscosity, it can be inserted in the channel with a syringe. Once cured for about one hour at $100 \text{ }^\circ\text{C}$, the epoxy solidifies irreversibly and can be used as a resistive Joule heater with a typical resistivity $\rho \leq 5 \times 10^{-6} \Omega \text{ m}$. Specific designs are shown in Fig. 1b and c. With the geometry shown in Fig. 1c, we estimated the actual temperature difference across the sample channel to be $\Delta T \approx 0.08 \Delta T_0$.

The setup was first tested on a quiescent solution by filling the a sample channel ($w = 50 \mu\text{m}$) with fluorescent polystyrene particles (PS) of diameter $a = 477 \text{ nm}$, suspended in 100 mM NaCl brine and stabilized against coagulation by a surface layer of the non-ionic surfactant Triton X-100. Fluorescence images of the device, placed under an inverted microscope, were acquired every 5 s , and the fluorescence intensity averaged along the sample channel axis in the direction of the flow. The transversal concentration gradient induced by thermophoretic motion of the particles is obtained as a function of time from the numerical derivative of the intensity profile, normalized to the fluorescence intensity of a uniform sample of $c = 0.01$ with no temperature gradient. The left panel in Fig. 2 shows that, as predicted, the concentration profile reaches its stationary state exponentially, with a time constant τ that does not depend on the

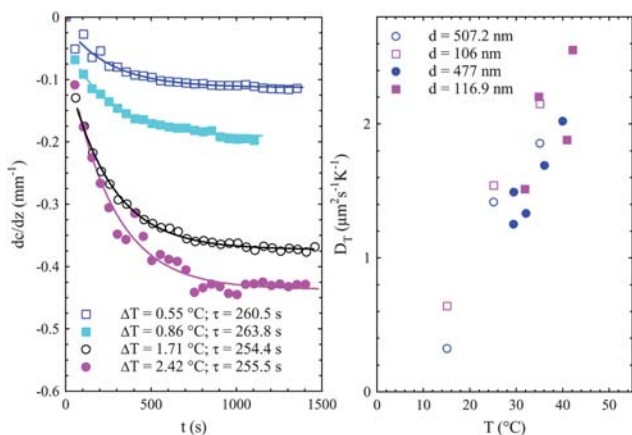


Fig. 2 Thermophoretic separation without flow. (Left panel) The concentration gradient as a function of time for a suspension containing sterically-stabilized fluorescent PS particles with a diameter $d = 477$ nm in 100 mM NaCl brine. The time constants τ obtained by an exponential fit to the curves are shown in the legend. (Right panel) Thermophoretic mobility D_T , was obtained using eqn (4) and τ , as a function of the average temperature (full symbols) compared to the data presented in ref. 26 (open symbols).

magnitude of ∇T and compares very well with the theoretical value $\tau = w^2/\pi^2 D \approx 250$ s for the particles we used. Using eqn (3), the asymptotic value of dc/dz allows evaluating the Soret coefficient of the suspension. The right panel in Fig. 2 shows that the values of S_T obtained at different average temperatures for these particles, and also for PS colloids with $a = 117$ nm, are in good agreement with the data reported in²⁶ for particles of similar size[†].

Flow measurements, aimed at evaluating the device as a microfluidic separator, were performed by feeding a sample channel of width $w = 75$ μm via a precision syringe pump (Harvard Apparatus), while the transverse temperature gradient was already established. Experiments were performed using flow rates of 0.01, 0.02 and 0.05 $\mu\text{L min}^{-1}$, corresponding to average velocities along the channel of about 90, 180 and 450 $\mu\text{m s}^{-1}$ respectively. Fluorescence images were acquired at 5 different positions along the channel, as shown in Fig. 3, averaged over 30 snapshots, and normalized to the intensity distribution without a temperature gradient.

Measurements were taken on devices exploiting both thermal designs sketched in Fig. 1a–b. Using an embedded ohmic heater, in this case, allows for designing longer flow paths (such as in Fig. 1c, where the sample channel is about three times longer) and therefore for using higher flow rates. In fact, assuming that the sample is flowing through a microchannel with velocity V , the constraint imposed by the diffusion time τ sets a minimum value

$$L_{min} \approx \frac{Vw^2}{\pi^2 D} \quad (5)$$

for the path length to achieve full separation. Using particles with $a = 477$ nm, the values of L_{min} corresponding to the three flow rates we used are about 5, 10, and 25 cm, so that, even using

[†] Note that, around room temperature, the ratio \tilde{D}_T/D varies between 0.5 and 2.5.

a sample channel length of 12 cm, there is only partial separation at the highest flow rate.[‡]

In passing, it is of note that the value of L_{min} , combined with the typical range for D_T , also sets an order or magnitude for the separation efficiency of a thermophoretic device per unit temperature difference and channel length. Indeed, if we measure L_{min} in units of the channel width, and call $\vartheta = \Delta T/T$ the fractional temperature difference, we can define a dimensionless “efficiency parameter”

$$\mathcal{E} \doteq \frac{\Delta c}{c(L_{min}/w)\vartheta} \approx \frac{\pi^2}{\text{Pe}_T} \quad (6)$$

where $\text{Pe}_T = wV/\tilde{D}_T = wV/D_T$ is a Peclet number associated to thermophoresis. For a channel width $w \approx 30$ μm , and values of V of the order of 10^2 $\mu\text{m s}^{-1}$, we have therefore $\text{Pe}_T \sim 1$ –10, and $\mathcal{E} = O(1)$.

As we stated in the introductory discussion, we want to show that particle drift can be tuned by changing the solvent electrolyte content. Recently, it has been theoretically predicted¹⁹ and experimentally observed²⁰ that the addition to a colloid of strongly mobile ionic species, such as H^+ or OH^- , yields distinctive thermoelectric effects, akin to the Seebeck effect in solids, which strongly affect particle thermophoresis. A qualitative explanation of the latter can be given by considering, for instance, an aqueous suspension of negatively-charged thermophobic particles, to which a simple base such as NaOH is added. The stronger tendency of the OH^- ions in accumulating to the cold side, compared to the Na^+ cations, generates a steady-state electric field, which counteracts particle drift. It is important to point out that, although the thermoelectric field remains finite, local charge separation vanishes in the macroscopic limit, so the experimental cell behaves basically as a lossy capacitor. More quantitatively, if we consider a monovalent electrolyte and impose local charge neutrality, then at steady-state the thermoelectric field is given by

$$\mathbf{E} = k_B \delta\alpha \nabla T \quad (7)$$

where k_B is the Boltzmann constant, $\delta\alpha = T[(S_T^+)^+ - (S_T^+)^-]/2$, and $(S_T^+)^{\pm}$ are the intrinsic Soret coefficients that cations and anions would have in the absence of charge coupling. [§] Such a thermoelectric field induces an additional electrophoretic particle drift that superimposes to thermophoretic particle motion, and can intensify or conversely hinder the latter, depending on the sign of $\delta\alpha$.

We have then contrasted the behavior of PS particles in the presence of NaCl and NaOH. This is because²⁸ $\delta\alpha_{\text{NaOH}} < 0$, the thermoelectric field hinders thermophoresis in NaOH, while in principle the opposite takes place in the presence of NaCl, since $\delta\alpha_{\text{NaCl}} > 0$. In practice, however, the effect of NaCl is very weak. Conversely, since $|S_T^+|$ is much larger for OH^- than for Cl^- ,²⁸ the addition of 100 mM NaOH is more than sufficient, as shown in Fig. 4, to *fully reverse* particle motion. Recently, performing

[‡] Note also that, given these flow rates and the low concentration of the suspensions we used, shear-enhanced diffusion effects²⁷ can be safely neglected.

[§] Of course, charge coupling leads to the same value $S_T^{\pm} = [(S_T^+)^+ + (S_T^+)^-]/2$ for the *observed* Soret coefficient of cations and anions, which is equivalent to say that there is no macroscopic charge separation.

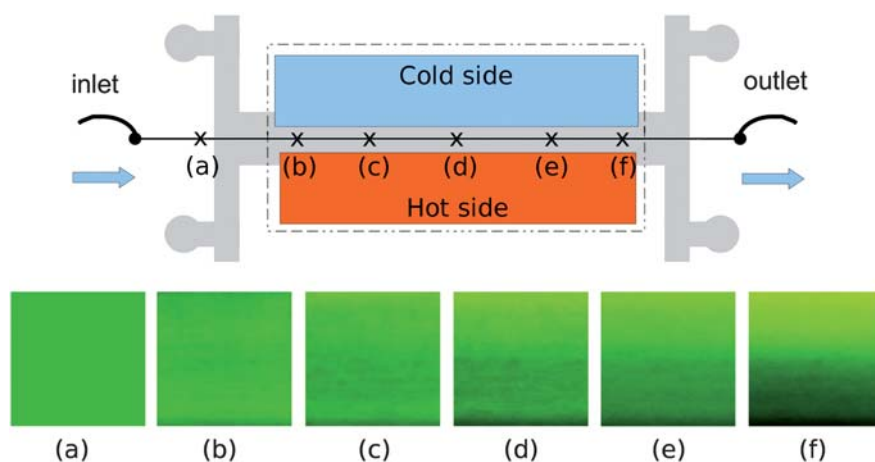


Fig. 3 Fluorescence images showing the accumulation of particles to the cold side. The experiment uses PS particles of 477 nm in diameter in the presence of 100 mM NaCl with a flow rate of $0.01 \mu\text{L min}^{-1}$.

similar measurements on charged micellar solutions by optical beam-deflection methods,¹⁶ Vigolo *et al.*²⁰ have shown that the particle charge can be obtained from the difference between the Soret coefficients obtained in the presence of NaCl and NaOH. A detailed study as a function of surfactant concentration, required to separate out the effects of interparticle interactions, actually yields a charge value that is consistent with what is predicted using effective charge considerations. In principle, a similar study could also be performed using microfluidic techniques for the latex particles we have used, but this is well beyond the scope of this paper. In addition, ref. 20 shows that the thermoelectric contribution can be finely controlled by working in mixtures of NaCl and NaOH, and tuning the mass fraction of NaOH at constant total ionic strength. Since the intrinsic thermophoretic

contribution depends on particle size, while the thermoelectric contribution is basically proportional to particle charge,²⁰ this feature may allow fractionating particles with equal surface charge but different size or, conversely, particles with similar size but different charge. In other words, manipulating colloidal suspensions in electrolyte mixtures may combine the capabilities of thermophoresis and electrophoresis. Further detailed measurements are however required to fully assess this opportunity, so that the former claim should just be regarded as a suggestion for future studies.

In conclusion, this study has shown that applying controlled thermal gradients on the microfluidic scale is fully feasible, and that separators based on standard soft lithography techniques may be manufactured easily. As a further bonus, microfluidic

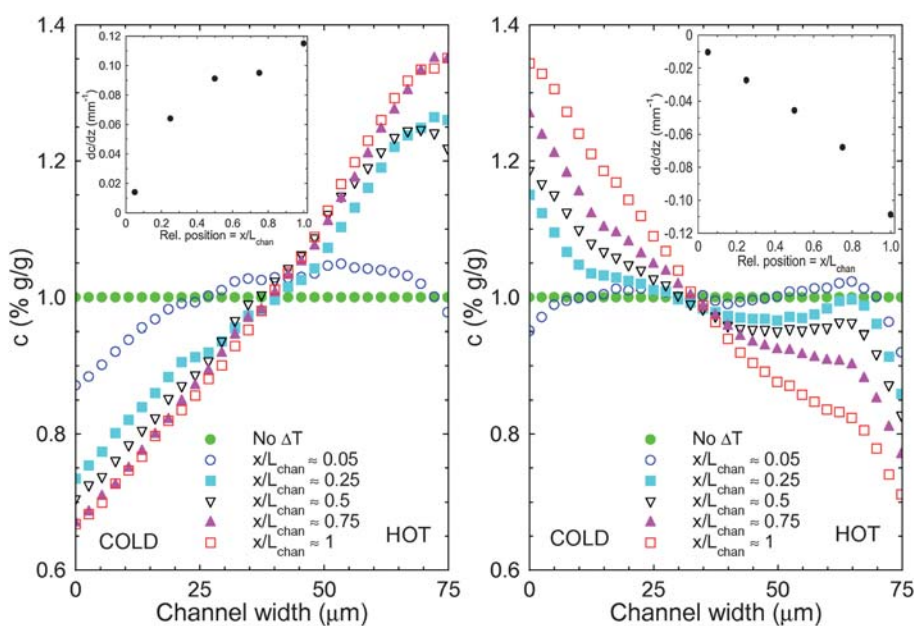


Fig. 4 A comparison between segregation effects for 477 nm PS particles in the presence of 100 mM NaOH (left panel), where particles accumulate to the hot side, and 100 mM NaCl (right panel), where the opposite takes place. In both graphs concentration profiles are measured, after the profile has reached steady-state, at 5 different positions along the channel. The particle concentration as a function of the relative position is shown in the two insets. Flow rate is $0.01 \mu\text{L min}^{-1}$.

devices may be extremely helpful to study thermophoresis of particles with large size. In this case, standard Soret measurements,[¶] are time consuming due to the long diffusion times.¹⁶ With respect to the prototypical devices that we have studied, a further reduction of the sample channel width would be helpful to enhance separation speed, which allows relaxation of the severe requirements for minimal channel length at high flow rates. In addition, improvements in terms of thermal control may be achieved by reducing the temperature drop across the PDMS layer between the side and the sample channels, for instance by reducing its thickness or by increasing its thermal conductivity by doping PDMS with dispersed thermally (but not electrically) conductive particles. More generally, our work suggests that any phoretic effect due to chemical potential gradients at the particle/solvent interface can be exploited in microfluidics. In this regard, it is useful mentioning a recent work by Abécassis *et al.*,²⁹ where salt gradients are used to drive particles and generate flow patterns in microfluidic channels by diffuso-phoresis.|| In comparison to the latter, thermophoretic methods allow for easier control and modulation of the interfacial driving force. Further advancements in thermal control and particle separation strategies in microfluidic devices are therefore to be expected.

References

- 1 C. Effenhauser, G. Bruin and A. Paulus, *et al*, *Electrophoresis*, 1997, **18**, 2203.
- 2 G. Bruin, *Electrophoresis*, 2000, **21**, 3931.
- 3 M. Becker, U. Marggraf and D. Janasek, *J. Chromatogr., A*, 2009, **1216**, 8265.
- 4 M. Hughes and *et al*, *Electrophoresis*, 2002, **23**, 2569.
- 5 C. Iliescu, L. Yu, F. Tay and B. Chen, *Sens. Actuators, B*, 2008, **129**, 491.
- 6 P. Gascoyne and J. Vykoukal, *Electrophoresis*, 2002, **23**, 1973.
- 7 B. Lapizco-Encinas, B. Simmons, E. Cummings and Y. Fintschenko, *Electrophoresis*, 2004, **25**, 1695.
- 8 B. Lapizco-Encinas, R. Davalos, B. Simmons, E. Cummings and Y. Fintschenko, *J. Microbiol. Methods*, 2005, **62**, 317.
- 9 F. Tay, L. Yu, A. Pang and C. Iliescu, *Electrochim. Acta*, 2007, **52**, 2862.
- 10 J. Shi, H. Huang, Z. Stratton, Y. Huang and T. Huang, *Lab Chip*, 2009, **9**, 3354.
- 11 C. Chang, Z. Huang and R. Yang, *J. Micromech. Microeng.*, 2007, **17**, 1479.
- 12 Y. Zhao, B. Fujimoto, G. Jeffries, P. Schiro and D. Chiu, *Opt. Express*, 2007, **15**, 6167.
- 13 T. Deng, M. Prentiss and G. Whitesides, *Appl. Phys. Lett.*, 2002, **80**, 461.
- 14 D. Inglis, R. Riehn, R. Austin and J. Sturm, *Appl. Phys. Lett.*, 2004, **85**, 5093.
- 15 K. Han and A. Frazier, *J. Appl. Phys.*, 2004, **96**, 5797.
- 16 R. Piazza and A. Parola, *J. Phys.: Condens. Matter*, 2008, **20**, 153102.
- 17 S. Iacopini and R. Piazza, *Europhys. Lett.*, 2003, **63**, 247.
- 18 S. Iacopini, R. Rusconi and R. Piazza, *Eur. Phys. J. E*, 2006, **19**, 59.
- 19 A. Würger, *Phys. Rev. Lett.*, 2008, **101**, 108302.
- 20 D. Vigolo, S. Buzzaccaro and R. Piazza, *Langmuir*, 2010, **26**, 7792.
- 21 D. Vigolo, R. Rusconi, R. Piazza and H. A. Stone, *Lab Chip*, 2010, **10**, 795.
- 22 P. Geelhoed, R. Lindken and J. Westerweel, *Chem. Eng. Res. Des.*, 2006, **84**, 370.
- 23 J. Janča, J. Berneron and R. Boutin, *J. Colloid Interface Sci.*, 2003, **260**, 317.
- 24 D. Duffy, J. McDonald, O. Schueller and G. Whitesides, *Anal. Chem.*, 1998, **70**, 4974.
- 25 J. McDonald, D. Duffy, J. Anderson, D. Chiu, H. Wu, O. Schueller and G. Whitesides, *Electrophoresis*, 2000, **21**, 27.
- 26 M. Braibanti, D. Vigolo and R. Piazza, *Phys. Rev. Lett.*, 2008, **100**, 108303.
- 27 R. Rusconi and H. A. Stone, *Phys. Rev. Lett.*, 2008, **101**, 254502.
- 28 J. Agar, C. Mou and J. Lin, *J. Phys. Chem.*, 1989, **93**, 2079.
- 29 B. Abécassis, C. Cottin-Bizonnel, C. Ybert, A. Ajdari and L. Bocquet, *Nat. Mater.*, 2008, **7**, 785.

¶ For instance performed by beam-deflection methods, where the inter-plate separation can hardly be smaller than a few hundreds microns.

|| Note that, at variance with the thermoelectric effects we have discussed, here no electric field is present. The driving mechanism is rather different, and is due to the overall dependence of the particle/solvent interfacial tension on the solute composition, which is not purely electrostatic. Indeed, diffuso-phoresis is noticeably salt-specific even for simple monovalent electrolytes.